

Search for high-frequency periodicities in time-tagged event data from gamma ray bursts and soft gamma repeaters

Adam T. Kruger,¹ Thomas J. Loredo,² and Ira Wasserman^{2,3}

ABSTRACT

We analyze the Time-Tagged Event (TTE) data from observations of gamma ray bursts (GRBs) and soft gamma repeaters (SGRs) by the Burst and Transient Source Experiment (BATSE). These data provide the best available time resolution for GRBs and SGRs. We have performed an extensive search for weak periodic signals in the frequency range 400 Hz to 2500 Hz using the burst records for 2203 GRBs and 152 SGR flares. The study employs the Rayleigh power as a test statistic to evaluate the evidence for periodic emissions. We find no evidence of periodic emissions from these events at these frequencies. In all but a very few cases the maximum power values obtained are consistent with what would be expected by chance from a non-periodic signal. In those few instances where there is marginal evidence for periodicity there are problems with the data that cast doubt on the reality of the signal. For classical GRBs, the largest Rayleigh power occurs in bursts whose TTE data appear to be corrupted. For SGRs, our largest Rayleigh power, with a significance of $\approx 1\%$, occurs in one record for SGR 1900+14 (at ≈ 2497 Hz), and in no other outbursts associated with this source; we thus consider it unlikely to represent detection of a real periodicity. From simulations, we deduce that the Rayleigh test would have detected significant oscillations with relative amplitude $\approx 10\%$ about half the time. Thus, we conclude that high frequency oscillations, if present, must have small relative amplitudes.

Subject headings: gamma rays: bursts — methods: statistical

¹Department of Physics, Cornell University, Ithaca, NY 14853

²Center for Radiophysics and Space Research, Cornell University, Ithaca, NY 14853-6801

³Floyd R. Newman Laboratory of Nuclear Studies, Cornell University, Ithaca, NY 14853-5001

1. Motivation

In the last decade observations of classical gamma ray bursts (GRBs) and soft gamma repeaters (SGRs) have finally identified the sites of the sources of these high energy transients, yet the physical nature of the sources remains mysterious (Paczynski 1995; Costa et al. 1997; Bond 1997; Djorgovski et al. 1997; Mészáros & Rees 1997; Horth et al. 1998; Frail et al. 1998; Taylor et al. 1998; Kulkarni et al. 1999). Detailed timing analysis of the high energy emission from these sources offers important clues regarding the nature of the central engines.

The positive detection of periodic emission in SGR flares suggests a rotating neutron star origin for these events, but to date, only two events have shown evidence of periodic emission (Barat et al. 1979; Cline et al. 1980; Terrell et al. 1980; Barat et al. 1983; Kouveliotou et al. 1999). The current picture of SGRs was first introduced in 1992 when it was proposed that they are neutron stars with extremely large magnetic fields, coined “magnetars” (Duncan and Thompson 1992). Part of the motivation for this model is the 8 s periodicity observed in the 5 March 1979 event, thought to be the rotational period of a neutron star associated with the source. In addition to rotation and precession, faster nonradial pulsations may be involved in the SGR events (McDermott, Van Horn and Hansen 1988; Duncan 1998). To date, no periodic emission has been detected from (classical) GRBs, but it might be expected at some level in some models. If binary compact stars or matter orbiting near neutron stars or black holes are involved in GRBs, it is likely that there are rapid, possibly periodic, associated phenomena. Quasi-periodic oscillations (QPOs) have been observed from accreting neutron star systems with frequencies as high as 1200 Hz. Some QPOs are thought to be associated with gas orbiting a neutron star at the innermost stable circular orbit at $r = 6GM/c^2$, where the Kepler frequency is $2200(M_\odot/M)$ Hz for a star of mass M ; for a black hole it may be as high as $11300(M_\odot/M)$ Hz. Recently, significant variability on time scales even shorter than 1 ms has been seen from Cen X-3, attributed to photon bubble oscillations that could produce quasiperiodic variability (Klein et al. 1996; Jernigan, Klein & Arons 2000). While it is presently unclear whether there are multiple classes of GRB progenitors, most plausible models involve a central black hole and a (temporary) debris torus around it. This includes massive progenitor systems, such as hypernovae or collapsars where a massive rotating star collapses to a black hole leaving behind an accreting disk of material that releases energy (Paczynski 1999; Nomoto et al. 2000), and many models involving the merger of compact stars. Short time scale variability, possibly including high frequency ($f \approx 10^3$ Hz) pulsations is expected for these types of sources, where material may be orbiting close to a nascent neutron star or black hole.

Further observation of periodic emission in SGR flares or detection of periodic emission from GRBs could provide valuable clues about the nature of the engines powering these

events. High-resolution, time-tagged data which makes a search for high frequency periodicities possible is available through the BATSE data archive at the Compton Observatory Science Support Center (COSSC).¹ We know of no other large-scale search for periodic emission that examines these data.

2. TTE data type

BATSE observed thousands of gamma ray bursts during the nine year life of the *Compton Gamma Ray Observatory (CGRO)*. In this study we analyze the BATSE Time-Tagged Event (TTE) data for 2203 GRBs and 152 outbursts from SGRs. The BATSE TTE data type consists of arrival times (with $2 \mu\text{s}$ resolution) for 2^{15} individual Large Area Detector (LAD) photon detection events for each detected burst. BATSE will generate a burst trigger if the count rate in two or more detectors exceeds a threshold specified in units of standard deviations above background (nominally 5.5). The rates are tested on three time scales: 64 ms, 256 ms and 1024 ms. TTE data is stored in a ring buffer that constantly records data from all eight LADs until a trigger. Once a trigger occurs, the most recent 1/4 of the buffer is kept, and the remaining 3/4 of the buffer is filled with events from the triggered detectors (or for the four highest rate detectors if more than four were triggered). In our analysis, we use data only from triggered detectors (i.e., we ignore some of the pre-trigger data). The TTE data type has the best time resolution of any BATSE burst data and thus provides the most precise information available about burst temporal behavior. Since burst intensities vary and TTE data is collected from a subset of the LAD detectors after trigger, the TTE data sets vary in time coverage and in number of arrival times from triggered detectors. In this study the number of arrival times analyzed from a single record varied significantly, with a maximum number of 29354. Under typical (non-burst) conditions the background gamma-ray photons are detected at a rate which fills the available buffer in about 2 s. In spite of this expectation, there are a number of TTE records which cover ≈ 3.75 s, and a few which last an anomalously long time ($\approx 7 - 8$ s). In the analysis we account for these variations to determine the significance of candidate periodicities.

In addition to these characteristics of the data sets, there is also significant variation in the burst profiles themselves evident from visual inspection of binned light curves. Some of the qualitative features of the light curves are useful for categorizing the data, such as the number of peaks and the fraction of the burst light curve covered by the TTE data. Since the buffer for TTE data is limited in size, many bursts are not fully covered. Since 1995 it

¹<http://coss.c.gsfc.nasa.gov/>

has been recognized that the distribution of T90 values for GRBs—the duration spanned by the central 90% of the burst photons—indicates two classes of bursts: one population with durations between 0.1 s to 2.0 s and another from 2 s to 100 s (Fishman & Meegan 1995). For our analysis we do not treat these populations separately. We do treat SGRs and GRBs separately, but we do not distinguish between long and short bursts.

The COSSC maintains an easily accessible collection of TTE data for short bursts.⁴ The collection is restricted to those bursts for which the TTE record covers the entire burst duration. It is possible that periodic emission occurs during burst precursors or the during the onset of bursts. For this reason we do not limit ourselves to TTE records that fully cover the burst; we obtain TTE data from the full COSSC FTP archive of BATSE data in FITS format. Also, for a small number of bursts, inspection of the TTE data by the COSSC team indicates that the triggered detectors were misidentified by the TTE hardware. For these triggers we have used only events from the true triggered detectors, which are sometimes limited in number. We note below some other rare anomalies among the TTE data.

3. The Rayleigh Test

The most widely-used procedure for determining which modes are present in a process such as photon emission is analysis of the power spectrum calculated from the discrete Fourier transform (DFT) of uniformly sampled data. Application of the DFT to arrival time series data requires binning of the data to produce equally spaced samples. Binning is a subjective procedure; choice of bin width can affect the apparent significance of a detection and limits sensitivity on short time scales. To avoid subjectivity and loss of sensitivity associated with binning, we use a procedure which does not require binning. We conduct our search for periodicities by using the Rayleigh power, R , as a test statistic (Mardia 1972; Lewis 1994; Mardia and Jupp 2000). The Rayleigh test was developed to detect a preferred direction in circular data (angles spanning $[0, 2\pi]$). For data such as the BATSE TTE data, one can assign to each datum a phase $\theta_i(f)$ given by

$$\theta_i(f) = [2\pi ft_i] \bmod 2\pi, \quad (1)$$

where the t_i are the photon arrival times and f is a candidate frequency. The Rayleigh power for a trial frequency f is calculated from the set of m photon arrival times $\{t_i\}$ by

$$R(f) = \frac{1}{m} \left[\sum_{i=1}^m \sin(2\pi ft_i) \right]^2 + \frac{1}{m} \left[\sum_{i=1}^m \cos(2\pi ft_i) \right]^2. \quad (2)$$

⁴<http://cossac.gsfc.nasa.gov/batse/batseburst/tte/>

(Note that there are two normalization conventions for R in the literature, the one we use, and one that divides our R by 2.) If one takes each event as defining a unit vector in the plane with components $(\cos \theta_i, \sin \theta_i)$, then mR is the magnitude of the sum of all the vectors. If there is a preferred phase present in the data, the sum will line up in the corresponding direction. If a particular set of measurements yield a resultant vector with a large magnitude for a particular choice of frequency, a periodic signal may be present at that frequency.

To quantify the evidence for a periodicity the Rayleigh test uses the Rayleigh power to test the null hypothesis that there is no preferred phase; i.e., that the distribution of θ_i is uniform. Under this hypothesis asymptotically $2R$ is the sum of the squares of two independent standard normal random variables with unit standard deviation and it follows that the random variable R is asymptotically distributed as χ_2^2 , so that the probability that R exceeds some threshold R_0 is

$$\text{Prob}(R > R_0) = e^{-R_0}. \quad (3)$$

If a single candidate frequency is specified a priori, equation (3) can be used to assess the evidence for a periodicity at that frequency. If the frequency is unknown, one must evaluate $R(f)$ at many trial frequencies to find the best candidate frequency (the one with the largest $R(f)$). The significance associated with the candidate frequency must account for the fact that many (possibly dependent) $R(f)$ values were examined. Finally, if one examines many data sets for evidence, the probability of finding a significant departure from the the predictions of the null simply due to chance increases. This must be taken into account when searching a catalog of events. We now discuss how we established a search strategy and how we accounted for the strategy in calculating significances.

4. Frequency search range and oversampling

In this section we will discuss how the 400 Hz lower bound for our frequency search was chosen and how the number and spacing of the frequencies searched affects the distribution of values of $R(f)$ expected from a burst record. For clarity we will refer to a particular event, BATSE trigger 6659, GRB 980326, which has been considered to be a hypernova candidate (Nomoto 2000). The light curve for this burst is shown in the inset to Figure 1.

For the results of the Rayleigh test to be meaningful, the null hypothesis must be a reasonable description of the data in the absence of a periodicity. One way to have uniform phases in absence of a periodicity is with a flat light curve, but this is not reasonable in this case. In our analysis, the uniform phase hypothesis is made reasonable through our choice of frequency search range.

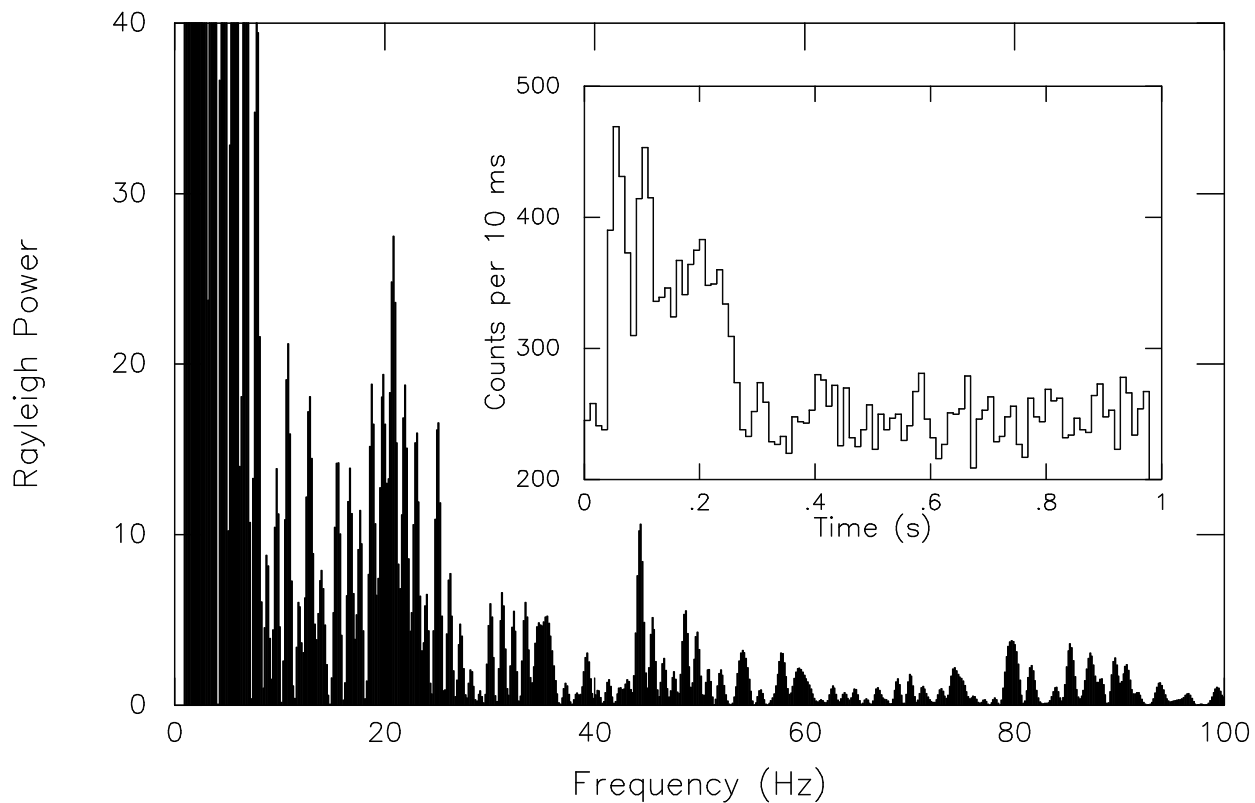


Fig. 1.— Power spectrum for BATSE trigger 6659 with frequencies sampled at rate 2π greater than the independent frequency sampling rate. This figure demonstrates how large calculated Rayleigh power can appear at low frequency due to long-timescale features of the burst. The light curve for this burst is shown in the inset with the photon arrivals binned in 10 ms bins. The onset of the burst is characterized by two brief spikes which result in a large power value near 20 Hz.

We note that the presence of the burst envelope can lead to large power values at frequencies corresponding to time scales in the envelope. Power due to major features of the burst can give an initial indication that there is some periodic component to the emission. This is apparent in the Rayleigh power spectrum shown in Figure 1. It is clear the large power at 20 Hz arises due to the two large spikes observed in the light curve at roughly 0.05 sec and 0.1 sec. This very large Rayleigh power does indicate that the photons do not come in uniformly during the observation time, but two spikes do not constitute a periodicity. We wish to avoid the influence of the burst envelope in our study. Figure 1 also shows that power due to the major burst features is evident out to frequencies of nearly 60 Hz, but at frequencies higher than this, the values are typical of background. Many of the bursts in our study have multiple narrow spikes, and for some of them power from the envelope extends to even higher frequencies. By examining the Rayleigh power for bursts in our sample at low frequencies, as well as for simulations of bursts with a smoothly varying envelope function modeled piecewise as a two-sided exponential, we set a conservative lower limit for our frequency search of 400 Hz. By choosing this lower limit we eliminate the power due to long-time structure in the burst envelope, and can use the Rayleigh test to search for high-frequency periodic emission with confidence. As a high-frequency cutoff for our search we chose 2500 Hz, a value just above the rotational break-up frequency for a ~ 10 km, $1.4 M_{\odot}$ neutron star.

In Figure 1 we have sampled the frequency axis at a rate 2π higher than if we limited ourselves to frequencies such that an integer number of periods is spanned by the data (Fourier frequencies). This provides us with a greater opportunity to observe large Rayleigh values if they are present since the peaks of $R(f)$ can lie between Fourier frequencies. The spike in the power spectrum near 20 Hz reaches 27.5, whereas calculations of power at only Fourier frequencies results in a maximum of 15.0. Under the null hypothesis, the significance level associated with a power of 27.5 is formally over 2×10^5 times smaller than that associated with 15.0. But more frequencies had to be examined to find the larger value, and this must be accounted for to assess its true significance.

If one examines only Fourier frequencies, the resultant powers will be statistically independent, but spacing of the samples may lead one to miss large values of the Rayleigh power. The benefits of higher resolution outweigh the significance penalty for oversampling. We chose to oversample using the same number of frequencies for each record. We compensate for this oversampling by determining an effective number of independent frequencies sampled using simulations. We have done this by finding the maximum value of the Rayleigh power achieved in our calculations of the power at 13194 frequencies between 400 Hz and 2500 Hz. Restricting ourselves to independent samples would lead to $2100T$ test frequencies, where T is the time coverage of the record, which is typically 1 – 3 s. We are thus over-

sampling by factors typically ranging from two to six (similar to recommendations in the literature, e.g., Lewis 1994). The probability distribution for the maximum power expected in such a search can be determined from the distribution for the power expected at a single frequency. We work out the form of this distribution in the next section.

5. Extreme value statistics

Our challenge in evaluating the evidence for periodic emission from GRBs and SGRs is to interpret the values of the Rayleigh power obtained from each non-repeatable burst event. Since we have designed our frequency search to avoid contamination by the slowly varying burst envelope, the (marginal) probability distribution for the Rayleigh power should be the same for each frequency in our search if there is no rapid oscillation of the source. Thus, for a particular burst record the most promising frequency candidate is the one at which the largest value of the power is found, R_{\max} . This maximum must be compared with the distribution of maxima expected under the null hypothesis of an uniform phase distribution.

In general, if we have N samples $\{x_i\}$, $i = 1$ to N , drawn independently from a probability density function $f(x)$ with a cumulative distribution function

$$F(x) = \int^x ds f(s), \quad (4)$$

and we have determined the largest of the x_i , X , then the probability distribution $g(X)$ for the extreme value X is (Ochi 1990)

$$g(X) = Nf(X)F(X)^{N-1}. \quad (5)$$

The most probable value of X can be found by solving

$$\frac{f'(X)}{f(X)} = -(N-1)\frac{f(X)}{F(X)}. \quad (6)$$

For the Rayleigh power, R , the cumulative distribution at a single frequency under the null hypothesis is $F(R) = 1 - e^{-R}$, and the density function is $f(R) = F'(R) = e^{-R}$. If R_{\max} is the maximum among N independent samples of R , its density is

$$g(R_{\max}) = Ne^{-R_{\max}}(1 - e^{-R_{\max}})^{N-1}. \quad (7)$$

Using (6) the most probable value of R_{\max} is

$$\hat{R}_{\max} = \ln N; \quad (8)$$

and

$$\begin{aligned} G(R_{\max}) &= \int_0^{R_{\max}} dr g(r) \\ &= (1 - e^{-R_{\max}})^N \end{aligned} \tag{9}$$

is the cumulative distribution for R_{\max} . For $Ne^{-R_{\max}} \ll 1$, $1 - G(R_{\max}) \approx Ne^{-R_{\max}}$.

The above analysis assumes the N samples are independent. When one is oversampling, this is not the case. But in such situations a good approximation to the extreme value distribution can often be found by using for N some number below the actual number of (dependent) samples; this is the *effective* number of samples. In our case, we sample 13194 frequencies for every record regardless of the duration, T , and number of events, n_{dat} in the record. We thus expect the effective number of frequencies sampled, N_{eff} , to vary from trigger to trigger as a function of T and n_{dat} .

In order to find a function which accurately describes this relationship a number of burst events were simulated varying T and n_{dat} , and N_{eff} was calculated by a maximum likelihood fit to simulation results for the number of (effectively) independent samples, N . The method used to simulate data is discussed in the next Section. For each simulated burst, i , we determine a maximum Rayleigh power $R_{m,i}$. The likelihood for the effective number, N , given the set $\{R_{m,i}\}$ is

$$\begin{aligned} \mathcal{L}(N) &= \prod_i^{N_b} g(R_{m,i}, N) \\ &= \prod_i^{N_b} Ne^{-R_{m,i}}(1 - e^{-R_{m,i}})^{N-1}, \end{aligned} \tag{10}$$

where N_b is the number of bursts or simulated events in our sample. We can determine the value of N which maximizes $\mathcal{L}(N)$; this is

$$N_{\text{eff}} = -\frac{N_b}{\ln[\prod_i^{N_b}(1 - e^{-R_{m,i}})]}, \tag{11}$$

the effective number of frequencies we use when calculating the significance of the maximum Rayleigh power.

We simulated sets of 100 burst events for 29 combinations of T and n_{dat} , and calculated N_{eff} for each. Figure 2 shows $N_{\text{eff}}(n_{\text{dat}})$ for $T = 1.1$ and $T = 2.0$ s. We can see that N_{eff} does not depend on n_{dat} systematically. Figure 3 shows the values of N_{eff} as a function of T for our simulations. The smooth curve is the best fit obtained for a functional form

$$N_{\text{eff}}(T) = N(1 - e^{-aT - bT^2}), \tag{12}$$

where N is the actual number of frequencies sampled and a and b are fit parameters found to be $a = 0.543$ and $b = 0.202$. The form of this equation was chosen to satisfy $N_{\text{eff}} = 0$ at $T = 0$ and $N_{\text{eff}} \rightarrow N$ as $T \rightarrow \infty$.

6. Simulations and detection

In this section we discuss the method used to simulate burst data and analyze simulated arrival times to better understand our ability to detect periodicities using the Rayleigh test. A commonly used model for burst light curves is the fast-rise, exponential decay (FRED) model. We adopt this basic form here and model a burst as a two-sided exponential function plus background, with some percentage of the flare or background modulated at a frequency f . The intensity function we use for simulations is

$$I(t) = \begin{cases} Ae^{\Gamma_1(t-t_p)}[1 + \varepsilon_1 \cos(2\pi f(t - t_p))] + B[1 + \varepsilon_2 \cos(2\pi f(t - t_p))] & t \leq t_p \\ Ae^{-\Gamma_2(t-t_p)}[1 + \varepsilon_1 \cos(2\pi f(t - t_p))] + B[1 + \varepsilon_2 \cos(2\pi f(t - t_p))] & t > t_p. \end{cases} \quad (13)$$

The input parameters are the record duration, T , time of peak intensity, t_p , flare amplitude, A , rise constant, Γ_1 , decay constant, Γ_2 , background amplitude B , pulsed fraction on flare, ε_1 , pulsed fraction on background, ε_2 , and the frequency of the periodic emission component f . In principle, we could have different frequencies and phases for signal and background; in simulations, we generally took either $\varepsilon_1 = 0$ or $\varepsilon_2 = 0$. For simplicity we choose the phase to be zero at $t = t_p$. This function is continuous across t_p where it reaches a maximum,

$$I(t_p) = A(1 + \varepsilon_1) + B(1 + \varepsilon_2). \quad (14)$$

The simulations that were done to determine the value of $N_{\text{eff}}(T)$ used data generated from a constant intensity function ($A = \varepsilon_2 = 0$). This was done after first verifying that the existence of a FRED-type flare did not affect the value of N_{eff} that we obtain. To establish this we generated 500 simulated burst records with roughly 29000 points each; assuming $T = 1.5$, $t_p = 0.4$, $A = 15$, $\Gamma_1 = 25.0$, $\Gamma_2 = 20.0$, and $B = 12$, and with no periodic component. The value obtained for N_{eff} using equation (11) from these bursts was $N_{\text{eff}} = 9856$. The calculation for simulated data arising from a constant intensity for the same duration and approximately the same number of accepted times led to $N_{\text{eff}} = 9299$. A similar calculation was done for $T = 0.5$ and the difference between the obtained N_{eff} values was less than 1% with the data derived from the constant intensity function leading to a larger value. These differences in N_{eff} are small and do not significantly change the formal significance levels one

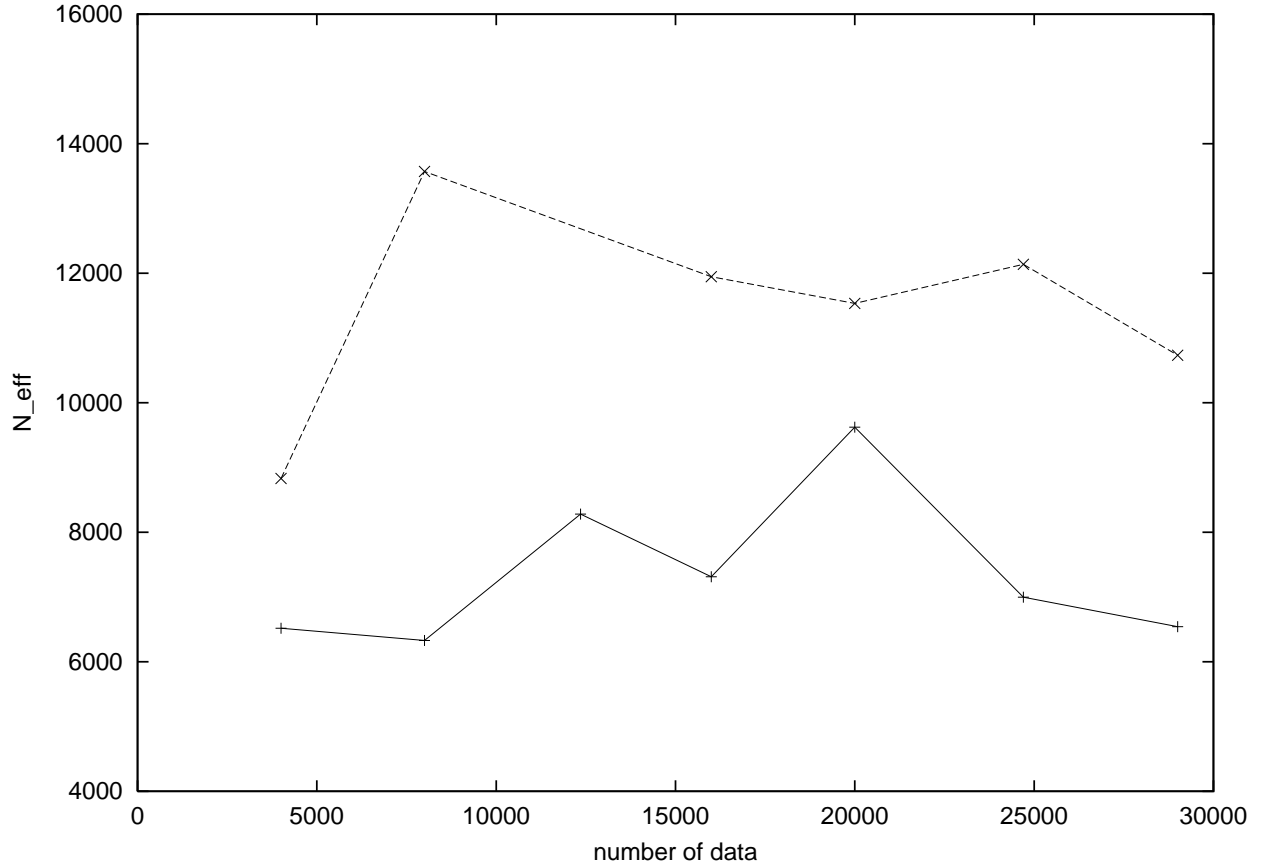


Fig. 2.— Calculated value of the effective number of frequencies sampled, N_{eff} , vs. the number of arrival times comprising the data record, n_{dat} , obtained from simulated data using a uniform rate function with duration, $T = 1.1$ s (bottom) and $T = 2.0$ s (top) and using 13194 frequencies from 400 Hz to 2500 Hz. There is no appreciable dependence of N_{eff} on the number of data n_{dat} .

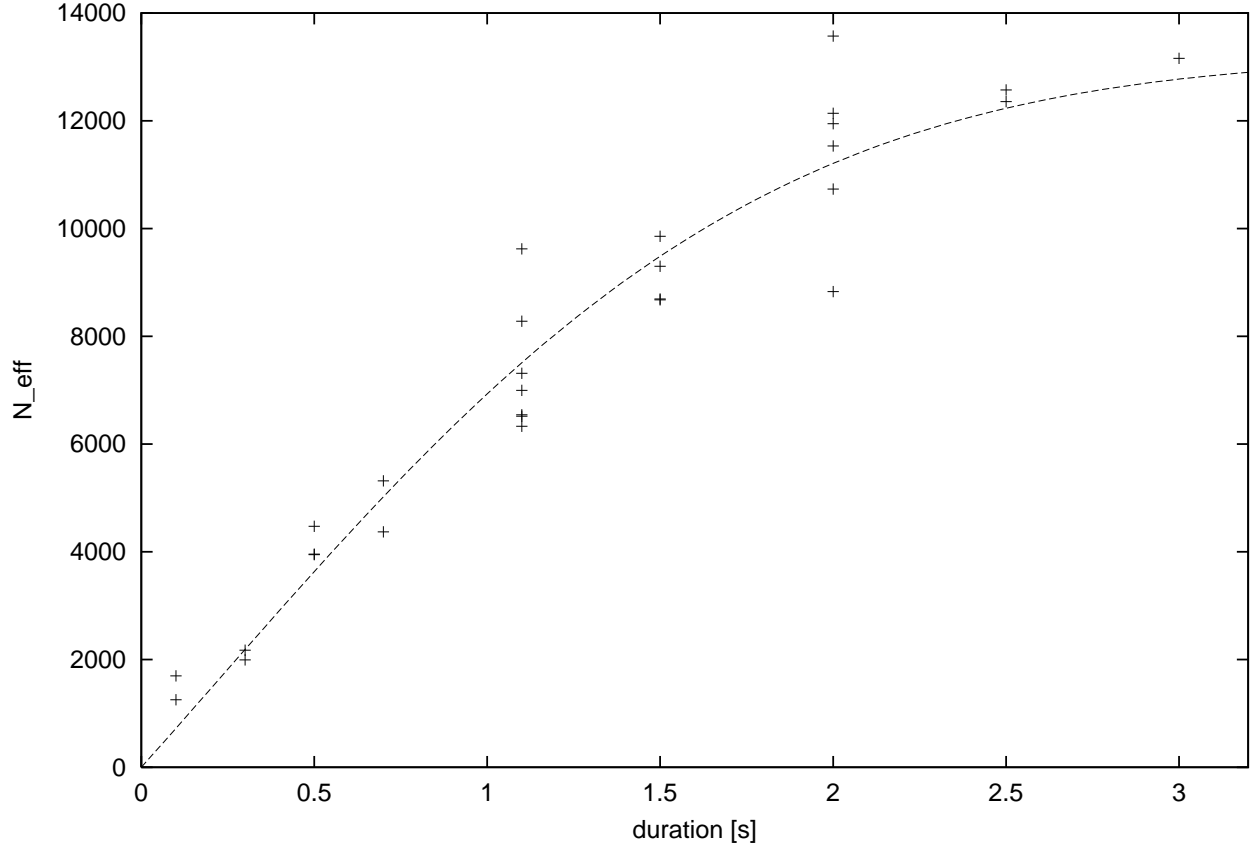


Fig. 3.— Effective number of frequencies sampled, N_{eff} , vs. record duration, T . Points obtained from simulated data using a uniform rate function and records with durations between 0.1 s and 3.0 s, and examining 13194 frequencies from 400 Hz to 2500 Hz. Plotted with best-fit function obtain from least squares fitting and 2 parameter model of the form, $N_{\text{eff}}(T) = N(1 - e^{-aT - bT^2})$, where $a = 0.543$ and $b = 0.202$ are the fit parameters.

would ascribe to an observed R_{\max} , justifying our use of the simplest null hypothesis for the calculations of section 6. This is not surprising given our previous finding that for frequencies above 400 Hz, typical burst envelopes do not change the expected power distribution from that found using a uniform phase distribution.

In addition to using simulations to establish expected distributions of R_{\max} values we can also use simulated data to establish how strong the periodic component in our model must be to be detectable. The significance of a particular maximum of the Rayleigh power is given by equation (15). We can use this expression and simulated data with a known input frequency and known pulsed fraction to determine what percentage of these records lead to maximum Rayleigh powers at a particular significance level. We did not anticipate that the results would depend on the value of the input frequency chosen, but to test this we have conducted simulations with two different input frequencies: 800 Hz and 2000 Hz. For each of these frequencies we generated 100 simulated data sets using equation (13) with $T = 2.0$, $t_p = 0.4$, $A = 20$, $\Gamma_1 = 10$, $\Gamma_2 = 10.0$, $B = 5.0$, $\varepsilon_2 = 0$, and $\varepsilon_1 = 0.07$, $\varepsilon_1 = 0.17$, and $\varepsilon_1 = 0.35$ and then searched the simulated data for periodicity. The corresponding pulsed fractions are 0.04, 0.10, and 0.20 respectively. In Figure 4 we show scatterplots of Rayleigh power vs. ε_1 for each set of 100 simulations. Figure 4(a) shows the results for an 800 Hz input frequency and Figure 4(b) shows results for 2000 Hz. Clearly when ε_1 (and hence the pulsed fraction on the flare) is increased the likelihood of a significant detection increases. With the input parameters chosen here and $\varepsilon_1 = 0.35$ (pulsed fraction of 20%), we find Rayleigh power values that would be considered statistically significant in all of the 200 simulations. A value of $\varepsilon_1 = 0.17$ (pulsed fraction of 10%) leads to significant detection in more than 50% of the trials. These simulations indicate that if the emission from a typical burst has an oscillatory component at the 10%-20% level, then the method that we employ here would allow us to confidently reject the hypothesis of a uniform distribution of phases and claim a significant signal detection (at the correct frequency) in a majority of cases. This conclusion does not appear to depend on the frequency of the oscillations, provided it is large enough.

7. Analysis

In this section we present the results of our analysis of the BATSE TTE data. In order to evaluate the evidence for periodic emission in the 2203 GRB and 152 SGR flare records in our study we have calculated the Rayleigh power for 13194 frequencies from 400 Hz to 2500 Hz for each trigger. Because we consider all frequencies equally likely a priori, the best candidate frequency is the one at which the maximum power is attained. In order to judge the significance of a particular R_{\max} value obtained from a burst record, we use the R_{\max}

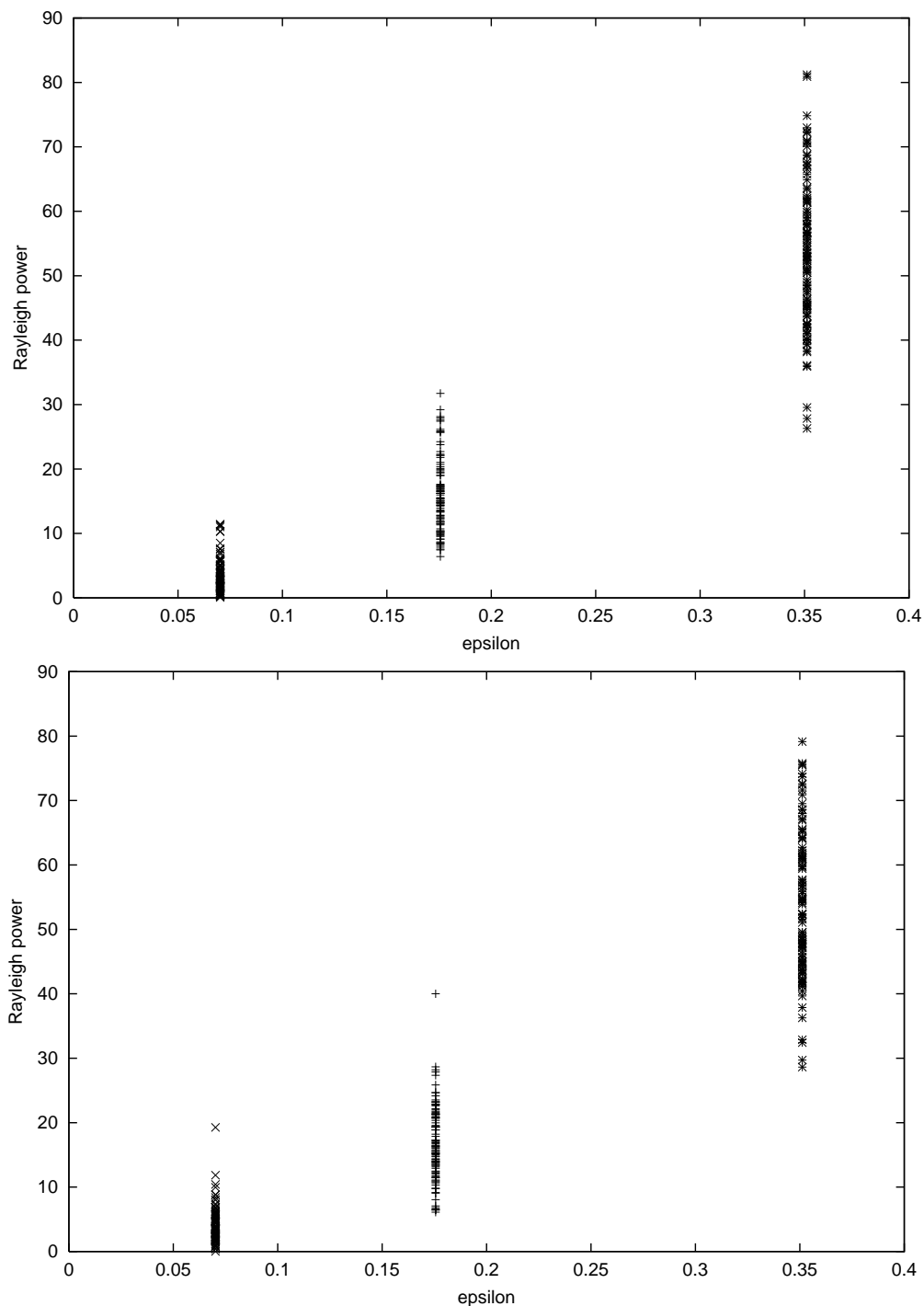


Fig. 4.— The Rayleigh power calculated at the input frequency in simulations vs. ε_1 of equation (13). The upper panel shows the power calculated for 800 Hz, and the lower panel shows the power calculated at 2000 Hz. These simulations demonstrate that with $\varepsilon_1 = 0.17$ (total pulsed fraction of 10%) we detect a signal with significance, $s \leq 1\%$ in more than half the trials, and for $\varepsilon_1 = 0.34$ (total pulsed fraction of 20%) we have significant detection at the correct frequency in 100% of the simulations.

distribution in equation (7). The tail area of this distribution is the probability of obtaining a larger value without the presence of a signal. The number of frequencies that enters this equation is given by equation (12) as a function of the time coverage T . Before doing our analysis we decided that we would keep the two populations of bursts, SGRs and GRBs, separate as they represent different classes of physical phenomena. We assign a score to each R_{\max} value, given by

$$s = 1 - (1 - t)^{N_b}, \quad (15)$$

where $t = [1 - (1 - e^{-R_{\max}})^{N_{\text{eff}}}]$, N_b is 152 for SGRs and 2203 for GRBs. This score is the significance that would be associated with R_{\max} were it the largest value in the population. This interpretation applies only to the single largest R_{\max} in each population, but s is useful more generally to identify potentially interesting events (those with small scores). Of the 2203 classical bursts in our study and 152 flares from SGR sources, only 4 led to Rayleigh powers high enough to have scores $s \leq 0.6$. Two of the records are GRB triggers, these are trigger 1493 with $R_{\max} = 15.85$ occurring at 819.0 Hz with $s = 0.54$ and trigger 2101 with $R_{\max} = 18.12$ found at 878.7 Hz and $s = 0.32$. The other two are SGR records: trigger 6855 with $R_{\max} = 16.78$ found at 872.0 Hz with $s = 0.10$, and trigger 7041 with $R_{\max} = 18.26$ occurring at 2496.7 Hz with $s = 0.01$. If one considers these results purely from the standpoint of statistical significance, it would seem that only trigger 7041 warrants additional attention, but more can be said about triggers 2101 and 6855.

The TTE light curve for trigger 2101 is shown in the inset of Figure 5. The most conspicuous feature of this trigger is a rapid drop in the number of counts recorded at around 0.7 seconds. No such feature is present in light curves produced using other (binned) BATSE data types for this event, indicating a problem with the TTE data for this burst. The TTE record begins with roughly 11000 photons that arrive at a rate consistent with background as observed in other records, roughly 20 per ms; but the rate falls abruptly to the anomalously low level of just one per ms. Because of the low count rate, TTE data exist out to 7 s. Because this record produced a very large Rayleigh score and the light curve revealed the odd change in count rate, we divided the record into two sections and calculated the Rayleigh power for each in an attempt to learn if the power arose from the first part of the record or the later low-rate portion. We find that the origin of the large Rayleigh power is the low-rate portion of the record. If we take all of the counts with $t > 0.75$ s and calculate the Rayleigh power spectrum we find the maximum to be at 902 Hz, with a Rayleigh power of 29.7 shown in the Figure, an extremely significant value. In addition to the peak at 902 Hz, there are other peaks with very large powers at other nearby frequencies, separated by roughly 10 Hz. It is unclear what causes these large values, but the anomalous feature of the TTE light curve indicates a serious problem with these data.

A distinguishing characteristic of this record is its long time coverage. In order to

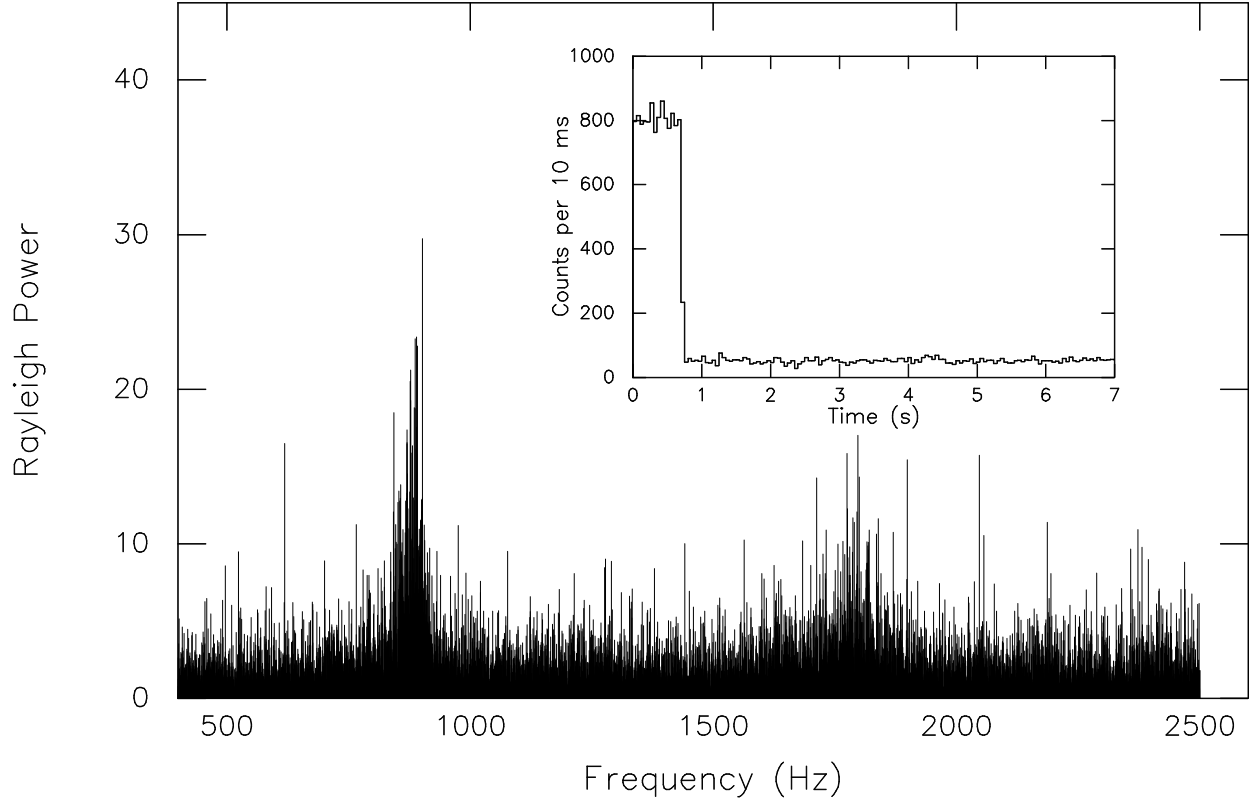


Fig. 5.— Rayleigh power as a function of frequency calculated for the low count rate ($t > 0.75$ s) portion of trigger 2101. Note the large power observed near 900 Hz and 1800 Hz. Similar power spectra were observed from other triggers where anomalously low count rates were recorded. The light curve generated from TTE data for this event is shown in the inset. Since this light curve is inconsistent with that produced from other archived data, we conclude that this set of TTE data is corrupted and that the large power here is not evidence of a periodic signal.

further study this phenomenon we searched the data sets for other records with atypical durations. We found among the GRB records four which have anomalously long coverage. The four GRB records occur in succession; they are triggers 2101, 2103, 2104 and 2105. Trigger 2102 had already been rejected from our study due to a problem with the data; the end of the record consists of many events all assigned the same arrival time. Inspection of the TTE light curves of the four GRB profiles indicates that each of them has the same basic appearance—a fast drop in count rate at about 1 s and in each case the TTE light curve bears no resemblance to light curves based on other BATSE data types. For each of these records we have separated out the low-count rate portion of the record and calculated the Rayleigh power at the frequencies in our search range. The results demonstrate that the source of the significant power in trigger 2101 is also present in the other records. We cannot say what the cause of this signal is, but we are confident that it is not astrophysical, and that the significant power that we find in these records does not constitute evidence of periodic emission from these GRBs.

One SGR record also has anomalously large time coverage of 6.5 s. This trigger is 6855, the burst with data leading to the second most significant maximum Rayleigh power among SGRs. Although the light curve obtained from this record did not reveal the rapid decrease in count rate found in the records mentioned above, we note that the record indicates a low count rate during the entire observation time. The frequency at which the power is a maximum is 872.0 Hz, similar to what we found in the problematic GRB triggers, 2101, 2103, 2104, and 2105.

The burst trigger from which we obtained the most significant evidence for periodicity in our study is trigger 7041. The light curve for this SGR outburst is shown in the inset in Figure 6. The burst is fully captured by the TTE data and there are no evident data anomalies in this record. The record for this burst contains 22383 arrival times and the time coverage is 1.0 s. The frequency which corresponds to the maximum Rayleigh power for this burst is 2496.7 Hz. Its Rayleigh power of 18.3 corresponds to a score of $s = 0.0124$; since this burst has the largest power, this score is the significance level. The source of this flare is SGR 1900+14, the same source that just 4 days before trigger 7041 produced a huge burst which was observed to have a 5 s periodicity (Hurley et al. 1998). This large flare was not captured by BATSE as the source was unfortunately occulted by the Earth at the time. There were 5 other triggers from SGR 1900+14 before 7041 but after the large flare of 27 Aug 1998, and 7 that followed in the subsequent 2 days. Because the maximum was obtained so near to our high-frequency search limit, and so near the large flare of 27 Aug, we were concerned that we might be missing large Rayleigh values in these other records by ending our search before finding them. To check this we extended our search to higher frequencies (up to 5000 Hz) for the triggers from SGR 1900+14 that occur after the large flare. In these

additional calculations we found no evidence for substantial power near 2497 Hz. Although the significance level associated with possible emission from trigger 7041 at 2496.7 Hz is interestingly small, and the folded light curve has a realistic appearance (Figure 7), we feel that this evidence is not strong enough to justify a claim of discovery of periodic emission. Other flares from the same source that occurred just before and soon after this trigger do not exhibit the same periodicity. We consider this record as an interesting oddity—a statistical anomaly rather than a bona-fide periodic signal.

8. Conclusions

This study is the first extensive search for high-frequency periodic emission to use the BATSE Time-Tagged Event data. The outcome of this study has not been the discovery of high-frequency periodicities in the burst records from SGRs and GRBs, but instead absence of evidence of these signals. In our study we have found just one plausible candidate for periodic emission at a frequency in our search range. The Rayleigh power obtained from trigger 7041 corresponds to detection near the 1% significance level, but the lack of emission at the same frequency in bursts from the same source (SGR 1900+14) at nearly the same time argues against this as a true detection. We have uncovered evidence for occasional TTE data corruption that produces a signal with $f \approx 900$ Hz; but the corrupt data is identifiable by obvious discrepancy between the TTE light curves and light curves using other data types.

We have simulated burst data in an effort to determine how strong a periodic component must be in the signal from a burst to be detectable. A rough rule-of-thumb is that for a catalogue with ≈ 2000 bursts, periodic modulation comprising $\approx 10\%$ of the photons in a given BATSE TTE record would have yielded significant Rayleigh power about half the time. (Since background is included in the record, the pulsed fraction in the burst signal must be higher.) Our analysis found oscillations at this level in only one TTE record, trigger 7041 from SGR 1900+14. That so few significant values of the Rayleigh power were found indicates that there is no substantial high-frequency periodic emission from these sources.

We gratefully acknowledge helpful conversations and correspondence about BATSE TTE data with Jay Norris, Jeff Scargle, and Jerry Bonnell. This work was supported by NASA grants NAG 5-3800, NAG 5-8356, and NAG 5-3427. This paper forms part of A. Kruger’s M.S. thesis at Cornell University.

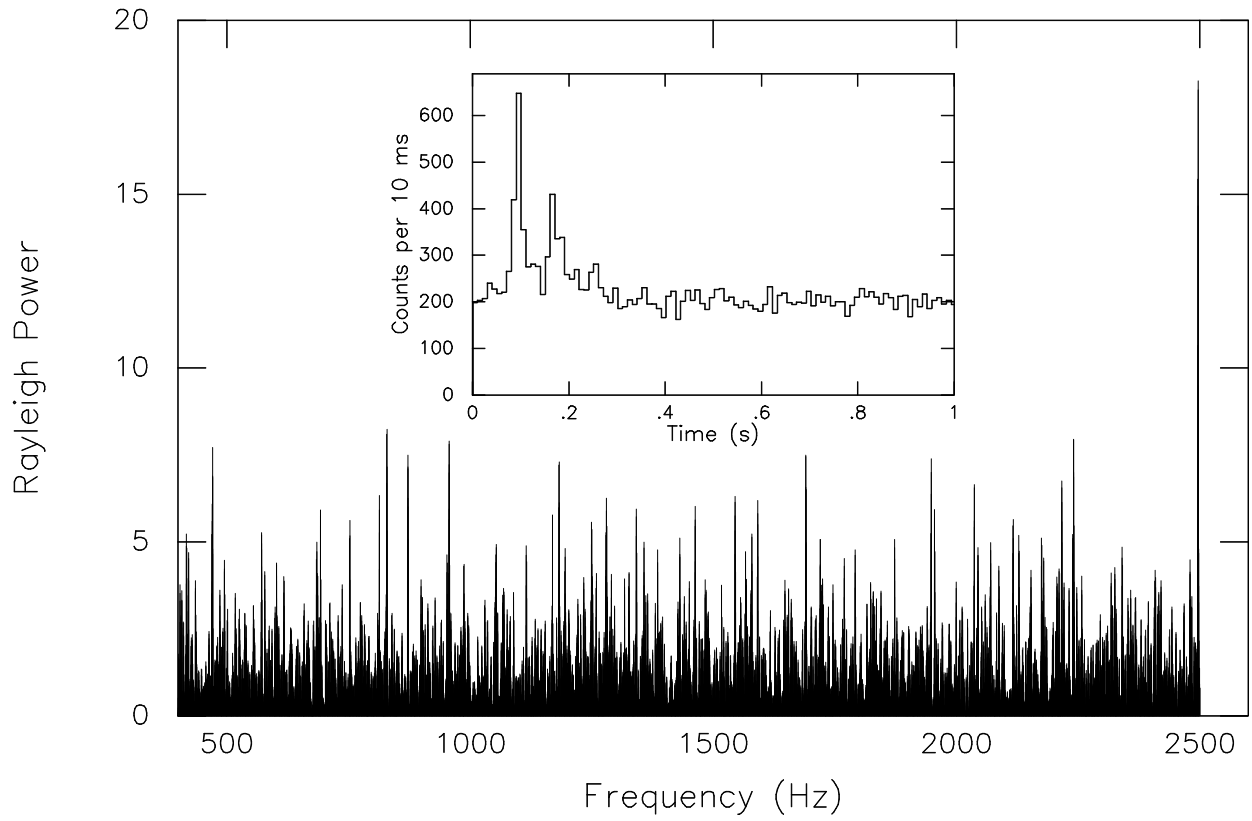


Fig. 6.— Rayleigh power spectrum for trigger 7041. A Rayleigh power of 18.3 is calculated for this trigger at 2497 Hz. This value results in a detection significance of 1.25% and is our most significant candidate periodicity.

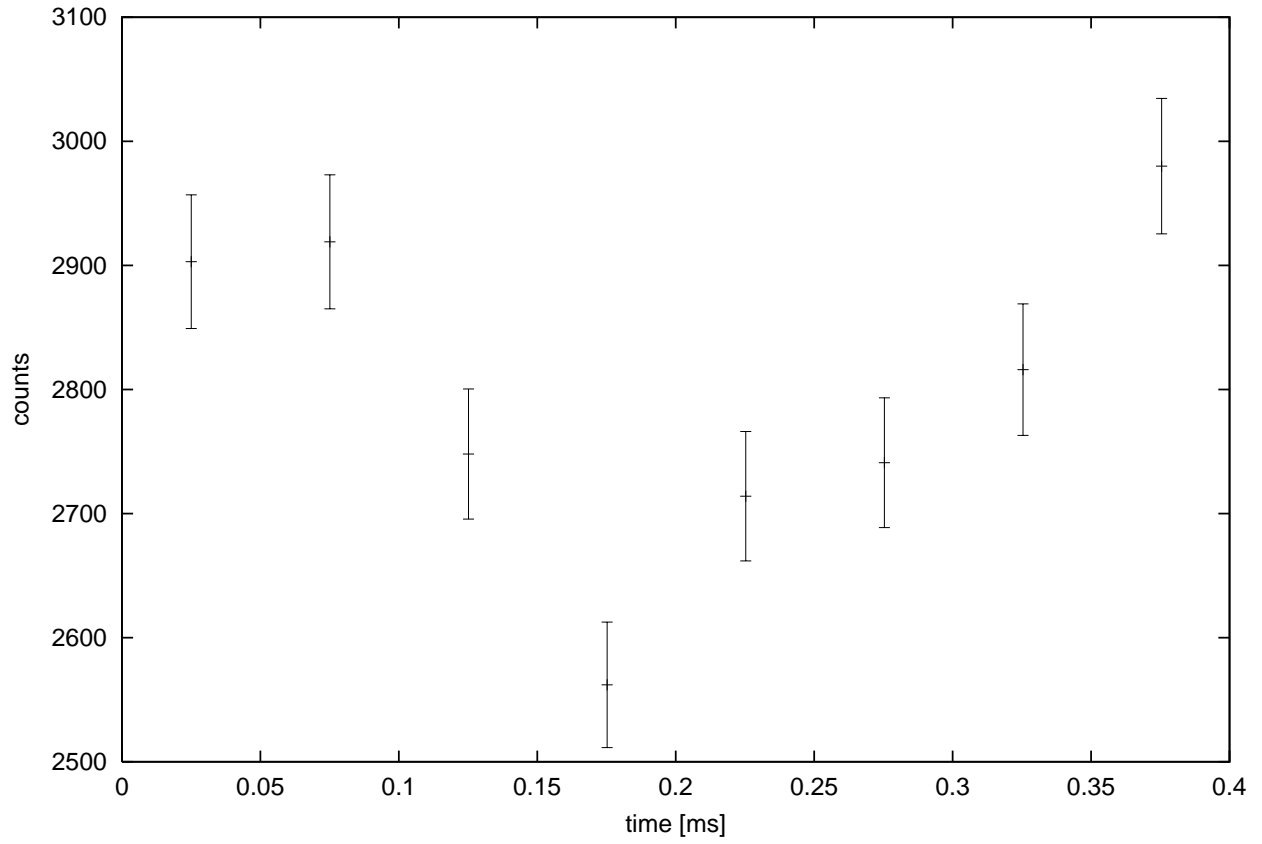


Fig. 7.— Folded light curve for data from trigger 7041 for frequency $f = 2497$ Hz (0.4 ms period). If there is a periodic component in this record, then the total pulsed fraction of the signal comprises roughly 10% of the data.

REFERENCES

- Barat, C. et al. 1979, A&A, 79, L24
- Barat, C. et al. 1983, A&A, 126, 400
- Bond, H. E. 1997, IAU Circ 6654
- Cline, T. L., et al. 1980, ApJ, 237, L1
- Costa E., et. al. 1997, Nature, 387, 783
- Djorgovski, S., et al. 1997, Nature, 387, 783
- Duncan, R. C. & Thompson, C. 1992, ApJ, 392, L9
- Duncan, R. C. 1998, in press (astro-ph 9803060)
- Fishman, G. J., & Meegan, C. A. 1995, ARA&A, 33, 415
- Frail, D. A., Halpern, J. P., Bloom, J. S., Kulkarni, S. R., & Djorgovski, S. G. 1998, GCN Circ. 128 (<http://gcn.gsfc.nasa.gov/gcn/gcn3/128.gcn3>)
- Hjorth, J., Andersen, M. I., Pedersen, H., Jaunsen, A. O., Costa, E., & Palazzi, E. 1998, GCN Circ. 109 (<http://gcn.gsfc.nasa.gov/gcn/gcn3/109.gcn3>)
- Jernigan, J. G., Klein, R. I., Arons, J. 2000, ApJ, 530, 875
- Klein, R. I., Arons, J., Jernigan, G., & Hsu, J. J.-L. 1996, ApJ, 457, L85
- Kouveliotou, C., et al., 1999, ApJ, 510, L115
- Kulkarni, S. R., et al. 1999, Nature, 398, 389
- Lewis, D. A. 1994, *Methods of Experimental Physics*, Chaper 12 (San Diego, Academic Press)
- Mardia, K. V. 1972, *Statistics of Directional Data* (London: Academic Press)
- Mardia, K. & Jupp, P. 2000, *Directional Statistics* (New York : Wiley)
- McDermott, P. N., Van Horn, H. M. & Hansen 1988, ApJ, 325, 725
- Mészáros, P & Rees, M. J., 1997b, ApJ, 482, L29
- Nomoto, K. et al., 2000 in *Supernovae & Gamma Ray Bursts*, eds. M. Livio et al. (Baltimore: STScI)
- Ochi, M. K., 1990, *Applied Probability and Stochastic Processes* (New York: Wiley)
- Paczynski, B. 1995, PASP, 107, 1167
- Paczynski, B., 1999 in *Supernovae & Gamma Ray Bursts*, eds. M. Livio et al. (Baltimore: STScI)

Taylor, G., Frail, D. A., Kulkarni, S. R., Shepherd, D. S., Feroci, M., & Frontera, F. 1998,
ApJ, 502, L115

Terrell, J. et al. 1980, Nature, 285, 587